



Role of Processing Temperature and Time on the Hydrothermal Alteration of K-Feldspar Rock in Autoclave

Davide Ciceri¹ · Marcelo de Oliveira¹ · Dennis P. Chen¹ · Antoine Allanore¹

Received: 10 February 2020 / Accepted: 4 May 2020 / Published online: 22 May 2020

© Society for Mining, Metallurgy & Exploration Inc. 2020

Abstract

Potassium fertilizers (potash) are mined in a handful of countries in the Northern Hemisphere. Potash is either expensive or unavailable to the farmers of the Southern Hemisphere. Alkaline alteration of K-feldspar rock (ultrapotassic syenite) in autoclave in the presence of Ca^{2+} generates a mixture of K-bearing calcium-aluminum-silicate-hydrate (C-A-S-H) minerals that potentially can be used as an alternative local fertilizer. This work investigates the effect of processing temperature (200 °C, 220 °C, and 230 °C) and time (from 0.5 to 3.0 h) on pH, mineralogy, and elemental availability of the C-A-S-H mineral mixture. Increasing temperature results in an increased conversion of K-feldspar and increased content of both the mineral tobermorite ($\text{Ca}_5\text{Si}_6\text{O}_{16}(\text{OH})_2 \cdot 4\text{H}_2\text{O}$) and amorphous phase in the resulting C-A-S-H mixture; increasing time results in an increased conversion of α -dicalcium silicate hydrate into tobermorite. The amount of K leached from the mixture is relatively constant across all processing conditions. Hydrothermal alteration in autoclave of K-feldspar-bearing rocks such as ultrapotassic syenite permits the synthesis of a potential potassium fertilizer which alkalinity and mineralogy can be tailored according to soil requirements.

Keywords Fertilizers · Hydrothermal processing · Potash · Calcium-aluminum-silicate-hydrate (C-A-S-H)

1 Introduction

Approximately 95% of the world market of potassium fertilizers (potash) is based on KCl. This soluble salt is largely mined in the Northern Hemisphere with Canada, Russia, and Belarus as the top producers accounting for more than 60% of the global output. In 2019, approximately 65 million tons of KCl were mined throughout the world. After mining, potash is transported via cargo ships to the Southern Hemisphere, according to established supply chains [1]. In the tropics, because of both distance from mining locations and limited local infrastructure, KCl is either expensive or unavailable. As KCl is highly soluble, it tends to be leached to the ground, providing limited benefits to tropical soils [2].

The need for a new class of affordable potassium fertilizers alternative to soluble salts for highly weathered soils has driven recent research. Non-evaporitic K-bearing minerals, for example K-feldspar, are globally distributed, and the K_2O content of ~5–10 wt% in their rocks makes them viable K resources alternative to KCl ores [3, 4].

The dissolution (weathering) and processing of K-feldspar are the subject of dedicated reviews [5–9]. In acidic soils, thermodynamics favors the weathering of K-feldspar to secondary minerals (e.g., clays). However, due to kinetic limitations, such processes are observed only at geological time-scales [4, 5, 10, 11]. The feldspar weathering rate under ordinary laboratory conditions ranges between 10^{-6} and $10^{-9} \text{ mol}_K \text{ m}^{-2} \text{ s}^{-1}$, and when compared to KCl, which has an infinitely fast dissolution rate, it is considered too low to fertilize crop growth. Therefore, affordable and environmentally friendly processing technologies are sought to enhance the rate of nutrient release to levels that can ensure profitable crop yields [2, 3, 6, 12–14]. Hydrothermal processing in autoclave can be used to accelerate chemical weathering. As an example, K-feldspar rocks (ultrapotassic syenite) and CaO processed hydrothermally in autoclave for 5 h at 200 °C and autogenous pressure (~14 atm.) resulted in a *hydrothermal material* with a calcium-aluminum-silicate-hydrate (C-A-S-H) mineralogy, basic pH, and multi-elemental release suitable

Electronic supplementary material The online version of this article (<https://doi.org/10.1007/s42461-020-00233-6>) contains supplementary material, which is available to authorized users.

✉ Davide Ciceri
ciceri@mit.edu

¹ Department of Materials Science and Engineering, Massachusetts Institute of Technology, 77 Massachusetts Avenue, Cambridge, MA 02139, USA

to improve acidic tropical soils [2, 15–17]. Thus far, the role of autoclave processing parameters on the degree of hydrothermal alteration of K-feldspar, resulting C-A-S-H mineralogy, and relationship to elemental leaching has not been reported in detail [18]. Although one could envisage that increased processing temperature and time promote the mineral alteration process in autoclave, the overall availability of nutrients from the processed hydrothermal material cannot be easily predicted given its multi-mineral composition. Particularly, K can be incorporated stochastically in the C-A-S-H phases that evolve over time during hydrothermal processing and the individual K release rate from each of these K-incorporating phases is currently unknown. Because the potential fertilizer value of the hydrothermal material for a specific soil and crop is tied to mineralogy, pH, and elemental availability, it is important to elucidate how such properties change as a function of processing parameters.

In this study, we investigate quantitatively mineralogy and elemental leaching of K-feldspar altered hydrothermally with CaO in autoclave, under a set of chosen processing temperatures (T) and processing times (t). Additionally, hydrothermal batches are synthesized at a scale of ~ 1 kg, which is a suitable production output for agronomic testing. The samples of hydrothermal material are characterized with X-ray powder diffraction (XRD), scanning electron microscopy (SEM), electron probe micro-analyzer (EPMA), and laser diffraction analysis of the particle size distribution (PSD). Leaching tests followed by inductively coupled plasma mass spectrometry (ICP-MS) of the leachate were also performed on the dried hydrothermal material obtained after processing in autoclave. This work shows that by modifying T and t independently during hydrothermal processing, it is possible to synthesize at a kilogram scale a potential potassium fertilizer which mineral content and pH properties can be tailored to specific soil and crop requirements.

2 Materials and Methods

2.1 Hydrothermal Processing

A sample labeled EBT13, an ultrapotassic syenite from the Triunfo batholith (Pernambuco State, Brazil), was used in this study. Briefly, the K-feldspar content determined by XRD was 79.5 wt% followed by albite (12.7 wt%) and pyroxene (6.6 wt%). The SiO_2 , Al_2O_3 , and K_2O content determined by XRF was 63.4 wt%, 17.1 wt%, and 13.4 wt%, respectively. The balance was mainly Fe_2O_3 (2.3 wt%), Na_2O (1.5 wt%), and CaO (1.1 wt%). Hand-sized field samples were comminuted in a jaw crusher and sieved through a 2-mm mesh. An in-depth characterization of the rock sample addressing chemical, mineralogical, and petrographic details is reported

elsewhere [4]. Note that this rock has a different composition than that used by Ciceri et al. [2].

CaO (reagent grade; Sigma-Aldrich) was used as received. An XRD scan showed that at the time of the experiment, the CaO grade was 94.5–97.0 wt%, with the main impurities being CaCO_3 (0.8–1.0 wt%) and $\text{Ca}(\text{OH})_2$ (2.2–4.5 wt%). Deionized water ($\kappa \leq 117 \text{ S cm}^{-1}$) was used for the synthesis of all hydrothermal batches.

The mixture used as a feed for the hydrothermal process was obtained by milling jointly in dry conditions 849.3 g of the ultrapotassic syenite and 150.8 g of CaO. The overall procedure was as follows: First, the rock was milled in a mild-steel ball mill (Rocklabs[®], $\phi = 20.32$ cm) for 5 min. Second, the rock powder after milling was screened through a sieve at 150 μm , and the material left on the sieve was milled again until it all passed through the 150- μm screen. Third, the powder $< 150 \mu\text{m}$ was co-milled with CaO for 5 min. The percentage of K-feldspar and K_2O in the feed mixture was 67.5 wt% and 11.4 wt%, respectively. The nominal molar ratio Ca:Si was 0.3, based on the assumptions of the absence of Ca minerals in the ultrapotassic syenite and 100% purity for CaO as discussed previously [2, 4]. For each of the hydrothermal synthesis, the feed mixture freshly prepared and water were loaded in a hydrothermal reactor also called autoclave (Parr Instruments, 7.6 L, Ti with stainless steel liner, 4843 Parr controller) at a weight ratio of 1:4, respectively. Processing was carried out in conditions considered relevant for industrial implementation, i.e., temperatures of 200 °C, 220 °C, and 230 °C and times from 0.5 to 3.0 h. A lower T does not yield a significant amount of available K; a higher T requires autoclaves that are likely to be too costly. For each of the chosen temperature and time, a new batch of feed mixture was processed for a total of 18 batches, each of 1 kg. The slurry obtained after processing each batch (i.e., solid material + supernatant) was poured in a pan and dried overnight at 120 °C. After drying, the solid cake was ground homogeneously with a pestle in an agate mortar for subsequent characterizations. Throughout the manuscript, this dried and re-ground sample is referred to as the *hydrothermal material*.

2.2 XRD

The XRD analysis was carried out with a Panalytical X'Pert MPD diffractometer. The analysis was run using the $\text{CuK}\alpha$ radiation as the X-ray source (45 kV; 40 mA). The 2θ -degree range for the scans was 6°–90°. The step size was 0.0131° with an accumulative counting time of 250 s per step. The quantification of the mineral phases was determined with the Rietveld refinement.

Further to a standard scan, for each sample, a second XRD scan was also run and the experimental parameters were the same as those of the first scan. However, for the second scan Si powder (NIST SRM 640) was mixed with the sample

(material:Si = 1:1). The Rietveld refinement on the second scan was used to compare the integrated intensity of the Si peaks and the integrated intensity of the known crystalline phases determined with the first scan. Differences in scattering power were considered in the procedure. The difference between the integrated intensities of the Si peaks and those of the other crystalline phases was considered to be the amorphous content. The final computed percentages of the crystalline components are the results of the first Rietveld refinement re-normalized to consider the amorphous component. As per our previous study [2], for all samples, a few small peaks estimated in the order of 1 wt% could not be identified and were not included in the analysis. Furthermore, samples showed a high degree of preferred orientation and overlapping peaks; thus, the Rietveld refinement required a great deal of manual fitting. XRD analysis results are estimates rather than accurate quantifications.

2.3 SEM and EPMA

The hydrothermal material was observed with the scanning electron microscope. Elemental point concentrations were made with the EPMA.

Imaging of the material was made by dusting a pinch of powder on conductive paint (Carbon Conductive Adhesive 502, Electron Microscopy Sciences). The SEM (JEOL 6610 LV) was operated in high vacuum mode ($< 10^{-3}$ Pa) using an accelerating voltage of 10–20 kV.

The point concentration determination was made on the sample mounted in thin sections (27 mm \times 46 mm; Spectrum Petrographics, Inc.). Before analyzing them, the sections were carbon-coated (Quorum, EMS 150T ES). The EPMA (JEOL JXA-8200) analysis was made with an accelerating voltage of 15 kV, a beam current of 10 nA, and a beam diameter of 1 μ m, and counting times on individual particles was 20–40 s. The same settings were applied to the X-ray elemental map, other than the current that was reduced to 1 nA.

2.4 Laser Diffraction PSD

The particle size distribution by laser diffraction was determined with LS 13 320 (Beckman Coulter, Inc.). The smallest particle size detectable with this instrument is 0.017 μ m.

The protocol followed the method ASTM C1070-01 [19]. For the analysis, samples were suspended in water without sonication or dispersant additives. Garnet.rf780z was chosen as the optical model, and density was assumed to be 2.6 g cm⁻³.

Laser diffraction measurements are a quick and efficient way to determine an entire PSD for comparison across batches of material. Oppositely, sieving can only provide an information of the type “larger than” or “smaller than” a given size threshold that is for the largest and smallest particles. A

commentary on advantages and disadvantages of different particle size techniques is given in ASTM E2651-19 [20].

2.5 Leaching Tests (Elemental Availability)

To determine the elemental availability from the dried material, particularly K, leaching tests were carried out. The leaching test is a separate procedure from hydrothermal processing. The rock was processed as described in Section 2.1 to generate a kg level of hydrothermal material. Then, for each of the hydrothermal batches, three subsamples of 0.3 g were leached to assess the elemental availability at room temperature and pressure as described in this section. The kilogram sample was thoroughly mixed to avoid segregations. A subsample of approximately 10 g was scooped out the main sample and subjected to coning and quartering until the desired final subsample of 0.3 g was obtained. The overall procedure was repeated three times to obtain three different final subsamples. Although such leaching experiments do not capture the dissolution behavior of the material in the soil, they allow a comparison of the elemental release across processed batches.

The leaching test was carried out according to the following protocol: First, a stock solution was prepared by appropriate dilution of standardized HNO₃ 0.1 M (Alfa Aesar) in water (Ricca Chemical Company[®], ACS reagent grade) to obtain the desired leaching solution, i.e., diluted HNO₃ at pH = 5. Second, 0.3 g of dried hydrothermal material was contacted with 3 mL of leaching solution.

After 24 h of agitation on a wheel rotator operating at 30 rpm, the leaching suspension was filtered (Whatman 13 mm GD/X, 0.45 μ m) and diluted 1:100 by volume in standardized HNO₃ 0.1 M. Filtering occurred within 15 min of stopping the rotation. Each of the leaching experiments was repeated in triplicates. The pH of all leachates after the 24 h under agitation was measured with a calibrated pH meter (Hanna, HI4222). Standard buffers used for calibration were at pH = 4.00 (Ricca Chemical Company[®]), pH = 7.00 (Ricca Chemical Company[®]), pH = 10.00 (Ricca Chemical Company[®]), and pH = 12.46 (Thermo Fisher Scientific). Lastly, ICP-MS was performed to determine the concentration of K, Al, Si, and Ca in the diluted leachate (ICP-MS; Agilent Technologies 7700 Series). The analysis used a 1 ppm solution of In as the internal standard (Sigma-Aldrich, TraceCERT[®]). Ca was determined in “no-gas” mode whereas the other elements were run with He at 4.0 mL min⁻¹.

3 Results and Discussion

3.1 Mineralogy and Imaging

Results from XRD analysis of the batches of hydrothermal material are shown in Fig. 1. Similar to previous studies with

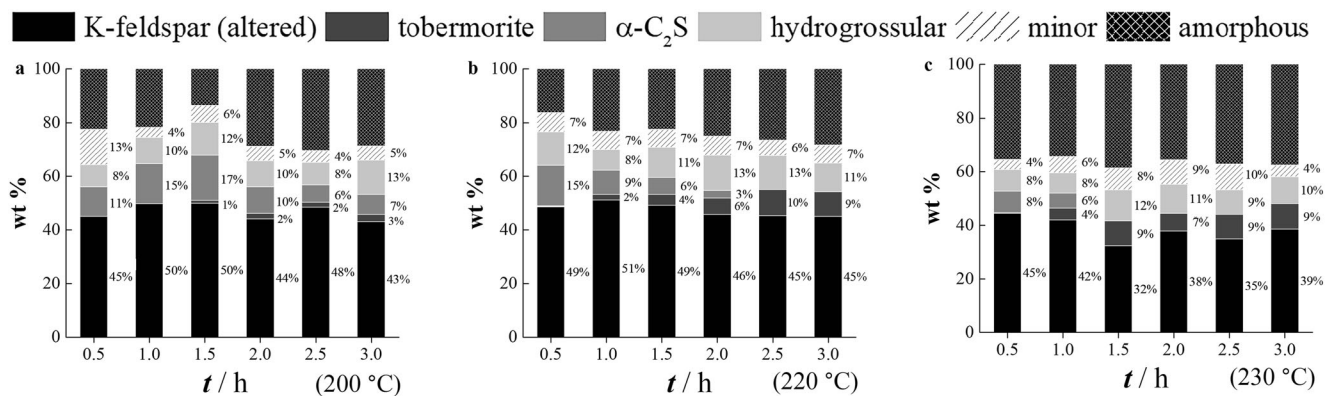


Fig. 1 X-ray powder diffraction (XRD) mineralogy of the dried hydrothermal material for increasing processing times (t) and temperatures (T). **a** 200 °C. **b** 220 °C. **c** 230 °C. “Minor” is the sum of minor phases, i.e.,

albite, biotite, panunzite, and quartz; for 200 °C-0.5 h minor phases, include also 4.8 wt% of portlandite $\text{Ca}(\text{OH})_2$

the same initial molar ratio Ca:Si of 0.3 [2, 15], the hydrothermal material contained K-feldspar (altered), hydrogrossular ($\text{Ca}_3\text{Al}_2(\text{SiO}_4)_{3-x}(\text{OH})_{4x}$), α -dicalcium silicate hydrate or α - C_2S in cement chemistry notation ($\text{Ca}_2(\text{SiO}_3\text{OH})(\text{OH})$, 11 Å tobermorite ($\text{Ca}_5\text{Si}_6\text{O}_{16}(\text{OH})_2 \cdot 4\text{H}_2\text{O}$), and a portion of minerals that did not significantly affect the C-A-S-H chemistry discussed here. These minerals were therefore grouped under the label of “minor phases” although they can reach a concentration up to 10 wt%. They included cryptoperthite albite (max 5–7 wt%) and, sporadically (max 1–3 wt%), biotite, panunzite, and quartz. Such phases were not confirmed by observations with the optical microscope and SEM. However, they were likely to be original components of the syenitic raw material [2, 4].

For the lowest T and shortest t (200 °C for 0.5 h), 4.8 wt% of $\text{Ca}(\text{OH})_2$ (portlandite) was also detected by XRD and included under the category of minor phases. An amorphous component was detected in all batches, with a maximum content of 38.6 wt% at 230 °C for 1.5 h. Selected point analysis of the chemical composition of the amorphous is reported in the [Supporting Information](#). The amorphous originates for the major part by the precipitation of calcium-silicate-hydrate (C-S-H) [21]. However, an increasingly disordered feldspar structure (i.e., the altered K-feldspar) may also be detected as amorphous by XRD. XRD did not detect carbonates in any of the samples [2]. Despite the limitations of XRD analysis [2], some trends are clearly identifiable in Fig. 1: (i) at 200 °C, the time required for CaO to react completely was at least 1 h, whereas at higher T , 0.5 h was sufficient; (ii) a 30 °C rise in T corresponds to $\sim 12\%$ increases in the time-averaged conversion of K-feldspar; (iii) the concentration of hydrogrossular in the hydrothermal material was relatively constant across all T and t (10 ± 2 wt% on average); (iv) increasing t transformed α - C_2S into 11 Å tobermorite, a transformation that was accelerated by increasing T from 200 to 220 °C; (v) increasing T from 200 to 230 °C increased the weight fraction of amorphous phase independent of t (24 ± 6 wt% at 200 °C and

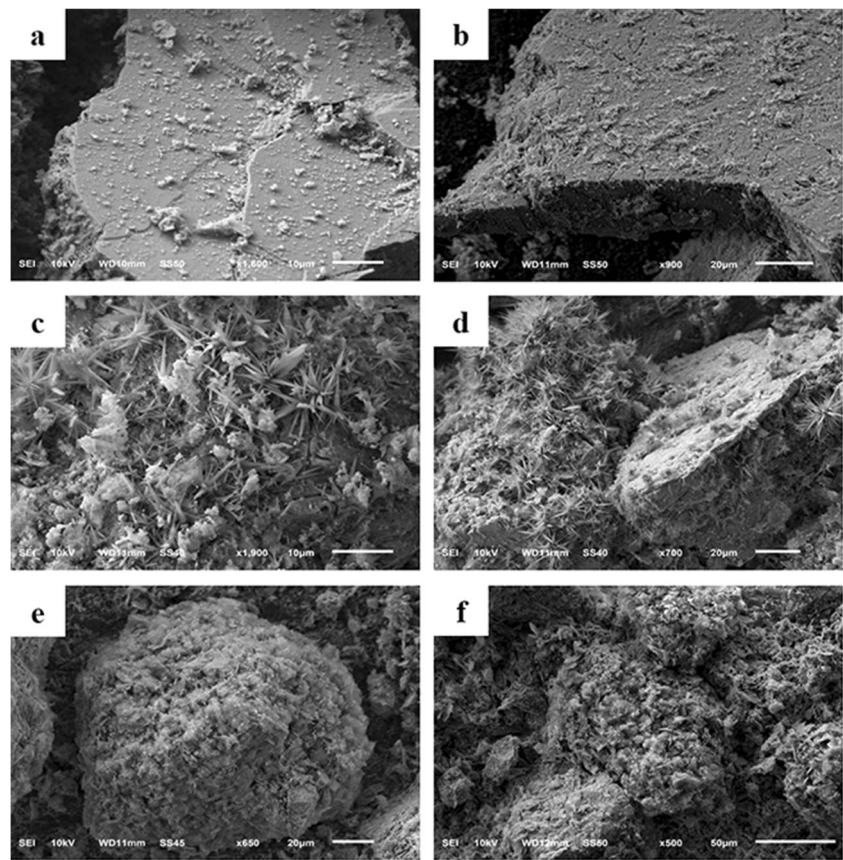
220 °C vs 37 ± 2 wt% at 230 °C), the amorphous content being inversely correlated to the fraction of altered K-feldspar; and (vi) the percentage of minor phases was constant across all T and t , in the order of 5–7 wt%.

Powder samples observed with SEM revealed key features of the hydrothermal material (Fig. 2). K-feldspar was severely altered, which was evident at all T , but more pronounced at 230 °C. Alteration included surface pitting and cracking (Fig. 2b). Additionally, point concentration analysis with EPMA ([Supporting Information EPMA](#)) confirmed chemical alteration, with particles of K-feldspar shown to be depleted in K and slightly enriched in Ca. C-S-H phases incorporated K even under the mildest processing conditions (200 °C for 0.5 h) ([Supporting Information EPMA](#) and [Supporting Figure S1](#)). At 220 °C and 230 °C, a characteristic needle-like structure attributed to well-crystallized tobermorite appeared in the material mounted in thin section, which became more common by increasing t . Tobermorite showed larger and better formed crystals than α - C_2S (Fig. 2c, d). Observation of crystal textures coupled with point analysis ([Supporting Information EPMA](#)) showed that α - C_2S converted into K-tobermorite by increasing t , in agreement with XRD results (Fig. 1). Both hydrogrossular and tobermorite were richer in Ca for samples processed at 220 °C rather than at 200 °C and 230 °C ([Supporting Information EPMA](#)). The underlying chemical reason is unclear. For samples processed at 220 °C and 230 °C, zeolites were also observed in thin sections ([Supporting Figure S2](#)) but not confirmed with other characterization techniques. As an example, zeolites were not detected by XRD, probably due to very low crystallinity, small crystal sizes ($< 10 \mu\text{m}$ and frequently $< 5 \mu\text{m}$), and concentration below detection limit.

3.2 PSD

The PSD for all samples is reported in Fig. 3. Data confirm previous findings, showing three distinct population peaks in

Fig. 2 Scanning electron microscopy (SEM) micrographs of **a** relatively pristine K-feldspar (200 °C for 0.5 h) and **b** pitted K-feldspar (230 °C for 3.0 h). **c, d** Needle-like structure attributable to tobermorite as observed at 200 °C and 200 °C for 2.0 h and 3.0 h, respectively. **e, f** Examples of agglomerates of intertwined tobermorite and amorphous compounds formed at the surface of K-feldspar particles at 230 °C for 2.0 h. XRD mineralogical composition of the samples imaged here is given in Fig. 1



the processed material, at ~100 to 50 μm, ~10 μm, and ~1 μm [2, 4]. The interpretation of the PSD peaks is flawed by the complex shape of the particles (Fig. 2), which is assumed to be spherical in the optical model used by the size analyzer. However, some general conclusions can still be drawn. The peak in the range ~100 to 50 μm is attributed to the fraction of altered K-feldspar, which would be dominant in this size fraction. At 220 °C and 230 °C, increasing *t* leads to a larger population of 10-μm particles that by comparing XRD (Fig. 1) and SEM (Fig. 2), can be attributed to aggregates of C-S-H phases such as tobermorite. The small shoulder between ~0.1 and ~1 μm is constant across all processing

conditions (Fig. 3) and could be attributed to hydrogrossular [2]. Complementary surface area measurements according to the BET method are reported in the [Supporting Information](#).

3.3 Elemental Leaching

Results from leaching experiments are reported in Fig. 4. The limitations of such experiments are discussed elsewhere [2]. Additionally, in this study, ~17 wt% of the feed mixture was constituted by an accessory mineral component from the syenitic rock [4]. Given that the reactivity of such a component was not resolved by XRD (Fig. 1), it may be a prominent

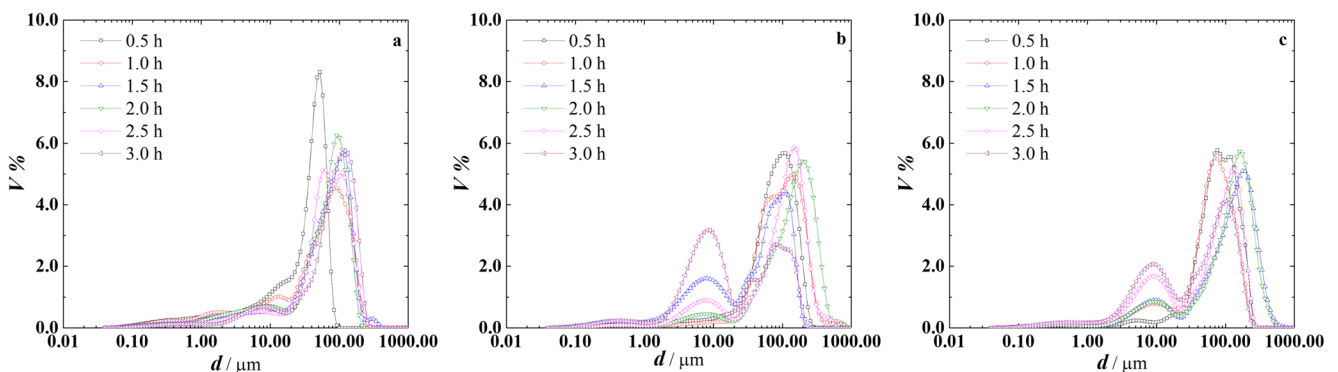


Fig. 3 Particle size distribution (PSD) of the samples of hydrothermal material processed at **a** 200 °C, **b** 220 °C, and **c** 230 °C for increasing processing times *t*

interference during leaching. As in our previous study, the pH of the leaching solution was not buffered [2], to avoid the formation of unwanted ion complexes or a chelating effect that may alter the dissolution behavior of the mineral phases. However, a limitation of such an approach is that the probed elemental availability may be the result of leaching pH rather than changes in the mineralogy of the material as a function of the processing conditions (Fig. 5). The actual pH of the leaching solution at 24 h (Fig. 5) is likely determined by the elusive soluble component (either KOH or K₂CO₃ species) that is present in the hydrothermal material although not detected by XRD [2]. However, C-A-S-H phases also play a role, as evidenced by comparison of XRD results (Fig. 1) with pH data (Fig. 5), which show the expected trend of decreasing pH with the decreasing molar ratio Ca:Si of the mineral phase being leached [22–24]. For the batch processed at $T = 200\text{ }^{\circ}\text{C}$ and $t = 0.5\text{ h}$, the actual leaching pH is ~ 12.6 due to the

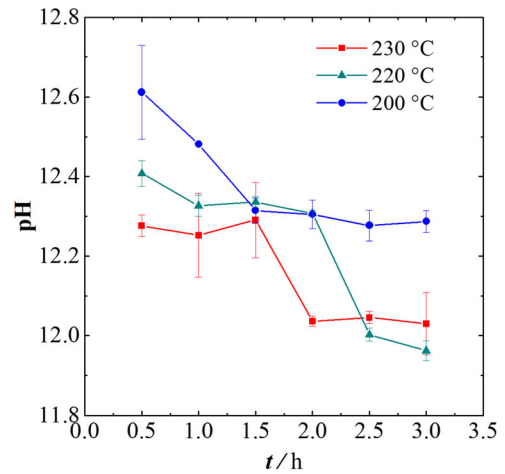


Fig. 5 Overview of pH values of the leaching solution after 24 h in contact with the hydrothermal material processed at different T and t . The x-axis is the processing time t

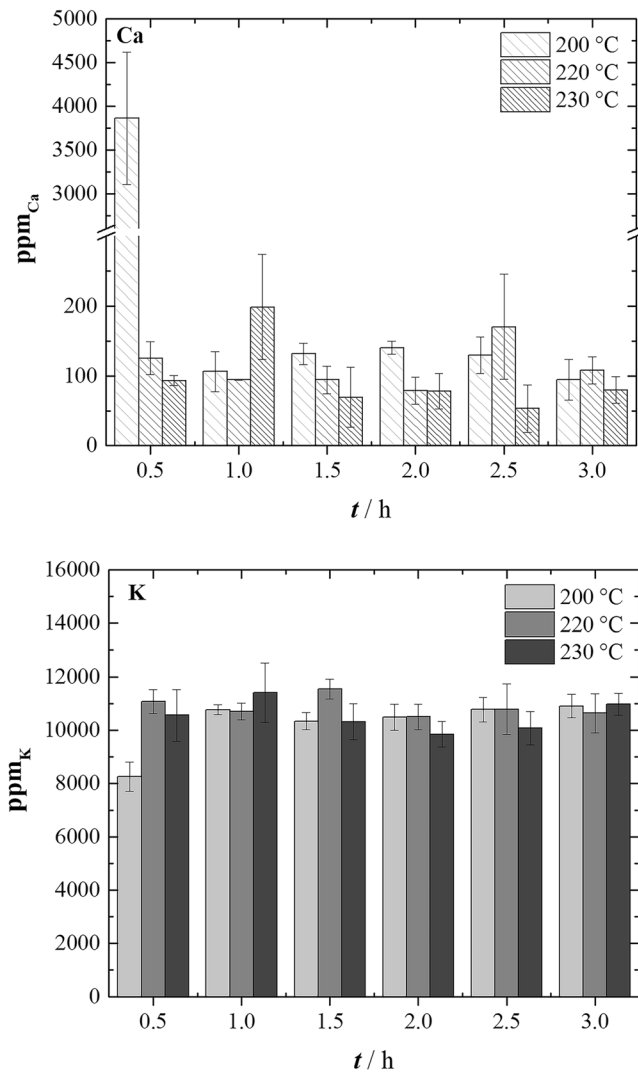


Fig. 4 Elemental leaching as a function of processing temperature (T) and time (t). Leaching conditions: batch test under rotation, 24 h, $m_S:m_L = 1:10$. HNO₃ at nominal initial pH = 5 and final leaching pH as shown in

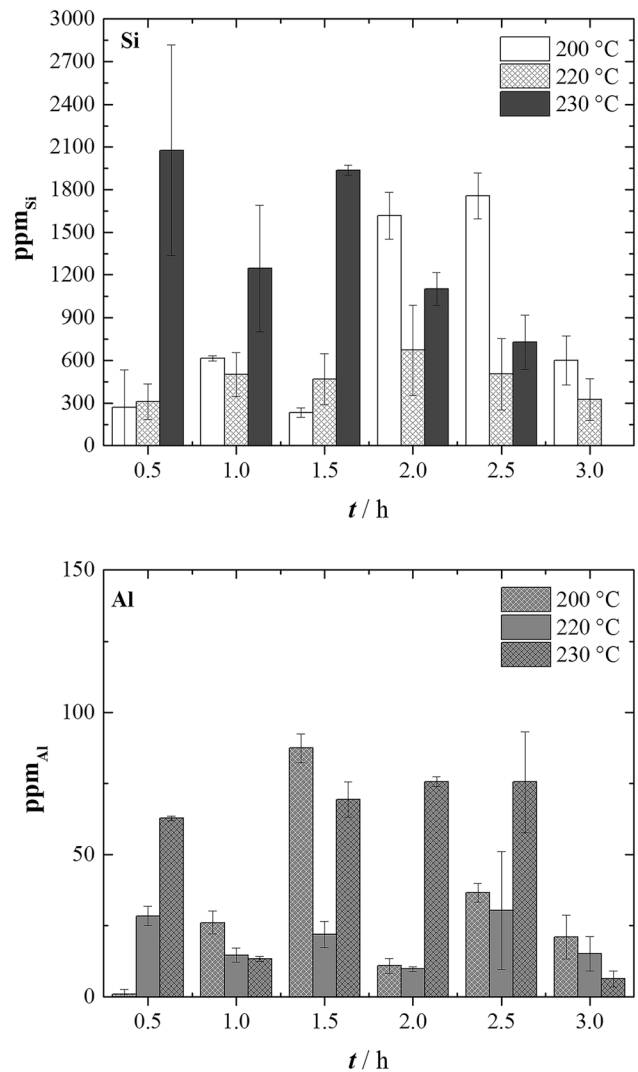


Fig. 5 All values (ppm) refer to the mg of element analyzed in solution by ICP-MS per kg of solid material. PSD and BET-SSA were different for each of the batches (Fig. 3; Supporting Information)

presence of portlandite (Fig. 1). For the same $T = 200$ °C, by increasing t , the pH value plateaus to ~ 12.3 , as dictated by the dissolution of $\alpha\text{-C}_2\text{S}$ during leaching. This behavior is confirmed in batches processed at higher T , which show again the same pH of ~ 12.3 as long as $\alpha\text{-C}_2\text{S}$ is present in the hydrothermal material. If processing is carried out for a sufficiently long time to allow the transformation of $\alpha\text{-C}_2\text{S}$ into tobermorite, the leaching pH decreases to a value of ~ 12 [22–24].

The availability of K is substantially unchanged across all sets of processing conditions (Fig. 4). An exception is the batch processed at 200 °C for 0.5 h, where the availability is significantly lower than that in other batches because not all of the $\text{Ca}(\text{OH})_2$ has reacted (Fig. 1). If such batch is excluded, the average availability corresponds to $10,683 \pm 433$ ppm of K in the solid material. If the focus is on K availability, processing can be considered accomplished within 1 h. From that point onwards, the dominant observation is the transformation of mineral phases such as $\alpha\text{-C}_2\text{S}$ transitioning to 11 Å tobermorite. At 230 °C, the conversion of K-feldspar was higher than 220 °C or 200 °C. However, this did not correspond to an increase in K leaching. As an example, even when altered K-feldspar constituted only 32.3 wt% of the hydrothermal material (230 °C for 1.5 h; Fig. 1), the K detected in the leaching experiment did not increase above the average. We consider some possible hypotheses to justify this behavior. The first hypothesis is that some of the K liberated during processing of K-feldspar is progressively incorporated in the C-A-S-H system, from which K would be released at a slow rate, making it less available during the 24-h leaching. Point concentration analysis with EPMA did not permit identifying clear trends but showed that both the amorphous and tobermorite did incorporate K, up to 10 wt% in some cases (Supporting Information EPMA). A complete digestion of the C-A-S-H, C-S-H, and amorphous phases was used to confirm an increasing K incorporation in such phases with increasing T (Figure S5 and Table S1), although not enough to justify XRD results. The second hypothesis is that XRD results are largely flawed by sampling, a high degree of material inhomogeneity that includes large disparity in particle sizes (Fig. 3) and coating of K-feldspar particles with C-A-S-H phases (Fig. 2; Supporting Figure S1) [2]. Additionally, altered K-feldspar although retaining a degree of crystallinity may be a disordered structure that would be detected by XRD in the “amorphous” fraction, further to the amorphous C-A-S-H or C-S-H. The K in this altered K would still be largely unavailable at the timescale of the leaching experiment, despite an increasingly disordered and altered structure. This hypothesis is partially supported by the fact that a truly higher conversion of K-feldspar should correspond to an increased formation of hydrogrossular given that neither the amount of Ca nor Si should be limiting in the processing of hydrothermal fluid. Experimentally, hydrogrossular is shown

to be approximately constant (Fig. 1). The third hypothesis is that the change in mineralogical composition detected by XRD is strongly biased by changes in the actual mass of material, which may change with processing conditions. If the mineral phases crystallize with and/or absorb at their surface a significant amount of water, the amorphous component would be overestimated. Although it may seem unrealistic that the material may contain up to 10 wt% of water, this hypothesis cannot be completely ruled out because previous batches processed at 200 °C have shown 5% weight loss on ignition [2]. All hypotheses may occur concurrently.

Ca is shown to be insensitive to both T and t , other than for the 200 °C, $t = 0.5$ h sample (Fig. 4) that contains portlandite (Fig. 1). The Ca that is available is only a small portion of the total Ca in the material.

Lastly, both Al and Si exhibit a pattern of difficult interpretation (Fig. 4). Al availability seems to be slightly higher at 230 °C than at lower T (Fig. 4), which may be due to the likely increased conversion of K-feldspar. For Si, the batches processed at 200 °C and 220 °C show a similar trend with respect to each other, with an increasing availability for increasing t up to 2 h, followed by a decrease for longer t . At 230 °C, the availability decreased by increasing t . Analytical error is significant for Si due to difficult determination with ICP-MS under the present experimental protocol.

Overall, key findings of the study are that for the given molar ratio $\text{Ca}:\text{Si} = 0.3$ in the initial feed, higher T and longer t lead to a higher conversion of K-feldspar and favor the formation in the final dried material of the cation exchanger 11 Å tobermorite with respect to that of metastable α -dicalcium silicate hydrate [15, 19, 25]. Despite an increased conversion of K-feldspar, the leaching of K observed is substantially unchanged across all processing conditions. However, to provide a more comprehensive interpretation of the entire dataset, a Spearman’s rank correlation coefficient analysis was performed (Supporting Information). Correlations coefficients summarize the trends highlighted in the preceding paragraph. There is a significant correlation between the amount of K-feldspar and $\alpha\text{-C}_2\text{S}$, which is the reflection of the formation of $\alpha\text{-C}_2\text{S}$ during the early stage of processing, when only a partial conversion of K-feldspar has occurred. This is also reflected in higher leaching pH. Conversely, K-feldspar is strongly anti-correlated to the tobermorite and amorphous content, which appear in the hydrothermal material at a more advanced conversion stage. The leaching of Ca and Al, which is very small with respect to the total content of these elements in the source material, does not appear to be correlated to any parameters. The leaching of Si is weakly, but statistically significantly, correlated to the amount of amorphous. It is demonstrated that several properties of the material can be tuned by modifying the underlining processing parameters. The amount of processed material was ~ 1 kg per batch as opposed to previous results (~ 25 g) [2]. Therefore, XRD and leaching

data demonstrate that the present process can be scaled to an output suitable for greenhouse or pot tests without compromising the key properties observed in smaller batches.

4 Conclusions

Hydrothermal processing of K-feldspar rock (ultrapotassic syenite) under alkaline conditions in autoclave generates a K-bearing material that is a potential source of K for agriculture. In this work, we investigated how processing temperature (T) and processing time (t) changed the C-A-S-H mineralogy of the hydrothermal material and its elemental leaching, given a molar ratio Ca:Si of 0.3 in the initial feed mixture. Additionally, we demonstrate that the process can produce kilograms of hydrothermal material. Increasing T and t increases the conversion of K-feldspar as detected by XRD and increases the fraction of tobermorite in the material, at the expense of α -dicalcium silicate hydrate (α -C₂S). The fraction of amorphous component increases by increasing T . Increasing T increased the K incorporated in C-A-S-H phases, although K leaching from the material was relatively constant across all T and t . Conversely, leaching of Al, Si, Ca (to an extent), and pH changes as a function of the processing conditions. The amount of Ca available in the leaching experiment and the pH are correlated with the amount of α -C₂S in the processed material. It is demonstrated that the mineralogy and pH properties of such a material can be modified through chosen processing conditions, which suggests the opportunity to adjust alkalinity and release of selected elements such as Si to meet specific soil requirements. Because the mineralogy and chemistry of the hydrothermal material underlie its potential fertilizer value, the data presented in this work allow for detailed agronomic and techno-economic analyses in the future.

Acknowledgments Hazen Research is acknowledged for carrying out the hydrothermal processing batches. Ms. Kaitlyn Hennacy is acknowledged for collecting the SEM images of Fig. 2. Dr. Steve Miller (H&M Analytics) is acknowledged for the collection of X-ray powder diffraction data and Rietveld refinements.

Availability of Data and Material Supplementary material includes EPMA dataset, EPMA elemental maps and micrograph of zeolites, BET surface area, digestion in sodium acetate buffer, and Spearman's rank correlation coefficient analysis.

Funding Information This work was supported by Advanced Potash Technologies.

Compliance with Ethical Standards

Conflict of Interest Advanced Potash Technologies, a commercial company, provided funding for this research in the form of salaries for the authors, equipment, and materials. The funder had no role in study design, data collection and analysis, decision to publish, or preparation of

the manuscript. The funder is developing a commercial product based on the research presented in this article. The funding of this work was subjected to the terms set forth by the Office of Sponsored Programs at the Massachusetts Institute of Technology (<http://osp.mit.edu>).

References

1. Yager DB (2016) Potash—a vital agricultural nutrient sourced from geologic deposits: U.S. Geological Survey OpenFile Report 2016–1167, 28 p., <https://doi.org/10.3133/of:20161167>
2. Ciceri D, De Oliveira M, Allamore A (2017) Potassium fertilizer via hydrothermal alteration of K-feldspar ore. *Green Chem* 19:5187–5202. <https://doi.org/10.1039/c7gc02633a>
3. Haseli P, Majewski P, Christo FC, Hammond B, Bruno F (2019) Thermochemical and experimental kinetic analysis of potassium extraction from ultrapotassic syenite using molten chloride salts. *Ind Eng Chem Res* 58(17):7397–7407. <https://doi.org/10.1021/acs.iecr.8b06328>
4. Ciceri D, de Oliveira M, Stokes RM, Skorina T, Allamore A (2017) Characterization of potassium agrominerals: correlations between petrographic features, comminution and leaching of ultrapotassic syenites. *Miner Eng* 102:42–57. <https://doi.org/10.1016/j.mineng.2016.11.016>
5. AAVV (1994). Feldspars and their reactions, NATO Science Series C
6. Ciceri D, Manning DAC, Allamore A (2015) Historical and technical developments of potassium resources. *Sci Total Environ* 502: 590–601. <https://doi.org/10.1016/j.scitotenv.2014.09.013>
7. Crundwell FK (2015a) The mechanism of dissolution of the feldspars: part I. Dissolution at conditions far from equilibrium. *Hydrometallurgy* 151:151–162. <https://doi.org/10.1016/j.hydromet.2014.10.006>
8. Crundwell FK (2015b) The mechanism of dissolution of the feldspars: part II dissolution at conditions close to equilibrium. *Hydrometallurgy* 151:163–171. <https://doi.org/10.1016/j.hydromet.2014.10.004>
9. Hongwen M, Yang J, Shuangqing S, Meitang L, Hong Z, Yingbin W, Hongbin Q, Zhang P, Wengui Y (2015) 20 years advances in preparation of potassium salts from potassic rocks: a review. *Acta Geol Sin* 89:2058–2071
10. Manning DAC (2010) Mineral sources of potassium for plant nutrition. A review. *Agron Sustain Dev* 30:281–294
11. Deer WA, Howie RA, Zussman J (2001) Framework silicates. Feldspars, 2nd edn. The Geological Society, London
12. Wilson MJ (2004) Weathering of the primary rock-forming minerals: processes, products and rates. *Clay Miner* 39:233–266. <https://doi.org/10.1180/0009855043930133>
13. Skorina T, Allamore A (2015) Aqueous alteration of potassium-bearing aluminosilicate minerals: from mechanism to processing. *Green Chem* 17:2123–2136. <https://doi.org/10.1039/C4GC02084G>
14. Wang C, Yue H, Li C, Liang B, Zhu J, Xie H (2014) Mineralization of CO₂ using natural k-feldspar and industrial solid waste to produce soluble potassium. *Ind Eng Chem Res* 53:7971–7978. <https://doi.org/10.1021/ie5003284>
15. Liu SK, Han C, Liu JM, Li H (2015) Hydrothermal decomposition of potassium feldspar under alkaline conditions. *RSC Adv* 5: 93301–93309. <https://doi.org/10.1039/C5RA17212H>
16. Liu S, Qi X, Han C, Liu J, Sheng X, Li H, Luo A, Li J (2017) Novel nano-submicron mineral-based soil conditioner for sustainable agricultural development. *J Clean Prod* 149:896–903. <https://doi.org/10.1016/j.jclepro.2017.02.155>
17. Ciceri D, Close TC, Barker AV, Allamore A (2019) Fertilizing properties of potassium feldspar altered hydrothermally. *Comm*

- Soil Sci Plant Anal 50(4):482–491. <https://doi.org/10.1080/00103624.2019.1566922>
18. Liu S, Han C, Liu J (2019) Study of K-feldspar and lime hydrothermal reaction: phase and mechanism with reaction temperature and increasing Ca/Si ratio. *Minerals* 9:46. <https://doi.org/10.3390/min9010046>
 19. ASTM (2020) C1070-01(2020), standard test method for determining particle size distribution of alumina or quartz by laser light scattering. ASTM International, West Conshohocken www.astm.org
 20. ASTM (2019) E2651-19, standard guide for powder particle size analysis. ASTM International, West Conshohocken www.astm.org
 21. Richardson IG (2008) The calcium silicate hydrates. *Cem Concr Res* 38:137–158
 22. Baston et al (2012) Calcium silicate hydrate (C-S-H) gel dissolution and pH buffering in a cementitious near field. *Mineral Mag* 76: 3045–3053. <https://doi.org/10.1180/minmag.2012.076.8.20>
 23. Glasser FP, Pedersen J, Goldthorpe K, Atkins M (2005) Solubility reactions of cement components with NaCl solutions: I. $\text{Ca}(\text{OH})_2$ and C-S-H. *Adv Cem Res* 17:57–64. <https://doi.org/10.1680/adcr.2005.17.2.57>
 24. Harris AW, Manning MC, Tearle WM, Tweed CJ (2002) Testing of models of the dissolution of cements - leaching of synthetic CSH gels. *Cem Concr Res* 32:731–746. [https://doi.org/10.1016/S0008-8846\(01\)00748-7](https://doi.org/10.1016/S0008-8846(01)00748-7)
 25. Houston JR, Maxwell RS, Carroll SA (2009) Transformation of meta-stable calcium silicate hydrates to tobermorite: reaction kinetics and molecular structure from XRD and NMR spectroscopy. *Geochem Trans* 10:1. <https://doi.org/10.1186/1467-4866-10-1>

Publisher's Note Springer Nature remains neutral with regard to jurisdictional claims in published maps and institutional affiliations.